

Spin-dependent Andreev reflection tunneling through a quantum dot with intradot spin-flip scattering

Xiufeng Cao, Yaoming Shi,* Xiaolong Song, and Shiping Zhou

Department of Physics, Shanghai University, Shanghai 200436, People's Republic of China

Hao Chen

Department of Physics, Fudan University, Shanghai 200433, People's Republic of China

(Received 10 January 2004; revised manuscript received 29 April 2004; published 30 December 2004)

We study Andreev reflection tunneling through a ferromagnet–quantum dot–superconductor system. The intradot spin-flip interaction is considered. By using the nonequilibrium Green function method, an expression for the linear Andreev reflection conductance is derived at zero temperature. It is found that competition between the intradot spin-flip scattering and the tunneling coupling to the leads dominates the resonant behaviors of the Andreev reflection conductance versus the gate voltage. A weak spin-flip scattering leads to a single-peak resonance. However, with the spin-flip scattering strength increasing, the Andreev reflection conductance will develop into a double-peak resonance indicating a novel structure in the conductance tunneling spectrum. Besides, the influences of the spin-dependent tunneling couplings, the Fermi velocity matching condition, and the spin polarization of the ferromagnet on the conductance are examined in detail.

DOI: 10.1103/PhysRevB.70.235341

PACS number(s): 73.63.Kv, 72.25.Dc, 74.50.+r

I. INTRODUCTION

With the advances in nanofabrication and material growth technologies, it has been possible to fabricate various kinds of hybrid mesoscopic structures.^{1–4} Recently, spin-dependent electronic transport through these hybrid mesoscopic structures has become one of the major focuses of the rapidly developing spintronics⁵ for both its fundamental physics and potential applications. In particular, the Andreev reflection (AR) in spin-polarized transport through ferromagnet–superconductor (F–S) junctions has been studied based on the scattering matrix formulation.^{6–11} It is found that at low bias voltage, the AR tunneling through the F–S interface is strongly affected by the spin polarization of the ferromagnet electrode,⁶ and the detection of the differential AR conductance can give information about the spin polarization at the Fermi energy for several metals.⁷ In addition, further investigations^{8,9} show that the AR conductance of the F–S junction is also modified by the Fermi velocity matching condition. For instance, the AR conductance may even increase first up to its maximum amplitude where perfect AR occurs and then drops quickly, indicating a nonmonotonic behavior with the spin polarization of the ferromagnet increasing. On the other hand, if one neglects the Fermi velocity matching condition, the effect of spin polarization invariably results in suppression of Andreev reflection.^{6,7}

On the other hand, spin-dependent resonant tunneling through a quantum dot (QD), a small system characterized by discrete electronic states, coupled with a ferromagnet (F) and a superconductor (S) forming a F–QD–S system, has been another interesting subject of experimental and theoretical investigations for the past decade. Zhu *et al.*¹² suggested an efficient method for writing spin in the F–QD–S system based on the AR-induced spin-polarization mechanism. They also studied the AR tunneling through a QD embedded in a three-terminal hybrid structure consisting of two ferromag-

nets and a superconductor by neglecting the intradot Coulomb interaction and the multilevel structure of the QD.¹³ It is found that the AR tunneling is strongly dependent, besides the spin polarizations and the matching condition of Fermi velocity, on the tilt angle between the magnetization orientations of the two F-leads. Feng and Xiong¹⁴ investigated the transport properties of an F–QD–S system, in which both the Coulomb interaction and the multilevel structure of the QD are considered. However, the spin-flip scattering effect being taken into account is confined to the tunneling barrier, and the intradot spin-flip scattering has not been involved yet.

The significant role of spin-orbit interaction in the QD, which may vary the spin orientation of an electron, has attracted considerable attention recently.^{15–19} The spin-flip mechanisms in the GaAs-based QD have been investigated in Ref. 15. Theoretical studies^{17–19} of the spin-polarized transport in magnetic nanostructures show that the intradot spin-flip scattering can lead to a novel spectrum structure in both the linear and nonlinear conductance of the F–QD–F systems in the Kondo regime. When the spin-flip scattering strength is comparable with the Kondo temperature, the original single Kondo peak in the differential conductance is split into a structure with two peaks or three peaks.^{18,19} Hence, it is natural to ask if the intradot spin-flip scattering could induce some novel spectrum of the AR conductance for such an F–QD–S system. This is an ongoing problem and, to our knowledge, no related reports have been found in the literature.

In this paper, we study AR tunneling through an F–QD–S hybrid structure by using the nonequilibrium Green function method. We mainly emphasize the effect of spin-flip scattering in the QD on linear AR conductance at zero temperature. The spin-flip scattering in the QD plays important roles in AR tunneling through the F–QD–S system. For an isolated QD, it can split one spin-degenerate level of the QD ε_d into two spin-coherent levels, $\varepsilon_{\pm} = \varepsilon_d \pm R$, whose states are a su-

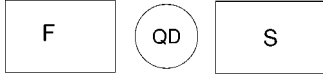


FIG. 1. The quantum dot with intradot spin-orbit interaction is coupled to a ferromagnet and a superconductor. A level of the QD is split into two spin coherent levels by the spin-flip interaction.

perposition of the spin-up and spin-down ones. Here R denotes the spin-flip scattering strength. It indicates¹⁷ that the incident electrons with up-spin and down-spin from the F-lead should tunnel coherently onto the levels split by the intradot spin-flip scattering. This spin-coherent tunneling process is expected to bring about some novel resonant features of the Andreev reflection conductance. Indeed, we found that the competition between the level splitting and the broadening of the split levels that arises from the tunneling coupling to the leads, together with the spin polarization and the Fermi velocity matching condition, can determine the spin-up and spin-down populations of the QD, thereby dominating resonant behaviors of the AR conductance of the system. When the spin-flip scattering strength overwhelms that of the tunneling coupling, the AR conductance versus the gate voltage displays a symmetric double-peak resonance, and the spin-flip scattering always suppresses the height of the double peaks. However, when a weak spin-flip scattering is involved, only a single peak exists in the AR resonant conductance. In this case, as the spin-flip scattering strength increases, the height of the single peak of the AR conductance may first increase gradually and then drop fast, depending on the matching condition of the Fermi velocity.

II. THE MODEL AND FORMULA

Consider the AR tunneling through a QD with the intradot spin-flip scattering connected to the F- and S-lead, in which only one spin-degenerate energy level is included and the Coulomb repulsion is neglected for simplicity. The spin quantization axis of the F-QD-S system is taken as the orientation of the F-lead magnetization, that is, the z axis. The model is shown schematically in Fig. 1. The Hamiltonian of the system under consideration can be written as

$$H = H_F + H_S + H_{dot} + H_T \quad (1)$$

with

$$H_F = \sum_{k,\sigma} (\varepsilon_{k\sigma} + \sigma M) f_{k\sigma}^\dagger f_{k\sigma}, \quad (2)$$

$$H_S = \sum_{p,\sigma} \varepsilon_{p\sigma} S_{p\sigma}^\dagger S_{p\sigma} + \sum_p (\Delta^* s_{p\uparrow}^\dagger s_{-p\downarrow}^\dagger + \Delta s_{p\uparrow} s_{-p\downarrow}), \quad (3)$$

$$H_{dot} = \sum_{\sigma} \varepsilon_d d_{\sigma}^\dagger d_{\sigma} + R(d_{\uparrow}^\dagger d_{\downarrow} + d_{\downarrow}^\dagger d_{\uparrow}), \quad (4)$$

$$H_T = \sum_{k,\sigma} (T_{k\sigma} f_{k\sigma}^\dagger d_{\sigma} + \text{H.c.}) + \sum_{p,\sigma} (T_{p\sigma} s_{p\sigma}^\dagger d_{\sigma} + \text{H.c.}), \quad (5)$$

where H_F and H_S are the Hamiltonians for the F-lead and the S-lead, respectively. Under the mean-field approximation, the F-lead is characterized by an internal magnetic moment \vec{M} . The tilt angle between the magnetic moment and the F-QD interface has been chosen to be zero. The BCS Hamiltonian is adopted for the S-lead with Δ the energy gap. H_{dot} models the QD with a single spin-degenerate level ε_d . The spin-flip term in the H_{dot} comes from the spin-orbit interaction in the QD (Refs. 15 and 17) and R is the spin-flip scattering strength. H_T describes the tunneling part between the QD and the F-lead/S-lead with the tunneling matrix elements $T_{k\sigma}$ and $T_{p\sigma}$. We have assumed that the spin of the electrons is conserved as the tunneling through the two side barriers of the QD, which is different from what is considered in Ref. 14.

The current flowing into the central region from the F-lead can be evaluated from the time evaluation of the total electron number in the lead,^{13,20}

$$J_I = -e \left\langle \frac{dN_I(t)}{dt} \right\rangle = -\frac{e}{\hbar} \text{Re} \sum_{k,i}^{i=1,3} T_{k,ii}^\dagger G_{k,ii}^<(t,t). \quad (6)$$

Here we express various kinds of Green functions in the 4×4 Nambu representation.²⁰ Let G^r denote the Fourier transformed retarded Green's function of the QD, and then G^r can be exactly solved in terms of Dyson's equation, $G^r = g^r + g^r \Sigma^r G^r$, in which g^r is the retarded Green's function for an isolated QD without the intradot spin-flip interaction, and Σ^r is the self-energy matrix due to both the tunneling couplings between the QD and the leads and the spin-orbit interaction in the QD. g^r can be easily obtained as

$$(g^r)^{-1} = \begin{pmatrix} \omega - \varepsilon_d + i0^+ & 0 & 0 & 0 \\ 0 & \omega + \varepsilon_d + i0^+ & 0 & 0 \\ 0 & 0 & \omega - \varepsilon_d + i0^+ & 0 \\ 0 & 0 & 0 & \omega + \varepsilon_d + i0^+ \end{pmatrix}. \quad (7)$$

For the F-QD-S system under study, Σ^r consists of three parts and can be written as $\Sigma^r = \Sigma_R + \Sigma_f^r + \Sigma_s^r$. The off-diagonal term of H_{dot} , i.e., the intradot spin-flip scattering contribution, is then conveniently expressed in terms of the self-energy Σ_R as

$$\Sigma_R = \begin{pmatrix} 0 & 0 & R & 0 \\ 0 & 0 & 0 & -R \\ R & 0 & 0 & 0 \\ 0 & -R & 0 & 0 \end{pmatrix}. \quad (8)$$

The spin-dependent tunneling coupling between the QD and the F-lead can be described by introducing the spin polarization P that specifies the F-lead magnetization. The spin-up and spin-down tunneling coupling strengths are defined as $\Gamma_{f\uparrow} = \Gamma_{f0}(1+P)$ and $\Gamma_{f\downarrow} = \Gamma_{f0}(1-P)$, respectively. The spin-averaged coupling strength Γ_{f0} denotes the tunneling coupling between the QD and the F-lead without internal magnetization, which is defined by $\Gamma_{f0} \equiv 2\pi\rho_f^n |T_{k\sigma}|^2$ with ρ_f^n being the density of states for the F-lead without magnetization. Under the wide bandwidth approximation, the self-energy coupling to the F-lead is $\Sigma_f^r = -(i/2)\Gamma_f$, where Γ_f is the tunneling coupling matrix between QD and the F-lead and is written as

$$\Gamma_f = \Gamma_{f0} \begin{pmatrix} (1+P) & 0 & 0 & 0 \\ 0 & (1-P) & 0 & 0 \\ 0 & 0 & (1-P) & 0 \\ 0 & 0 & 0 & (1+P) \end{pmatrix}. \quad (9)$$

The self-energy from the tunneling coupling between the QD and the S-lead Σ_s^r is given by

$$\Sigma_s^r = -\frac{i}{2}\rho_s^r(\omega)\Gamma_{s0} \begin{pmatrix} 1 & -\frac{\Delta}{\omega} & 0 & 0 \\ -\frac{\Delta}{\omega} & 1 & 0 & 0 \\ 0 & 0 & 1 & \frac{\Delta}{\omega} \\ 0 & 0 & \frac{\Delta}{\omega} & 1 \end{pmatrix}, \quad (10)$$

where $\rho_s^r(\omega)$ is the modified dimensionless BCS density of states,

$$\rho_s^r(\omega) = \frac{|\omega|\theta(|\omega|-\Delta)}{\sqrt{\omega^2-\Delta^2}} + \frac{|\omega|\theta(\Delta-|\omega|)}{i\sqrt{\Delta^2-\omega^2}} \quad (11)$$

and $\Gamma_{s0} = 2\pi\rho_s^n |T_{p\sigma}|^2$ is the tunneling coupling strength between the QD and the S-lead. ρ_s^n in Γ_{s0} is the density of states when the superconductor lead is in the normal state. It is useful to introduce the coupling matrix Γ_s to describe its tunneling to the S-lead,

$$\Gamma_s = \rho_s(\omega)\Gamma_{s0} \begin{pmatrix} 1 & -\frac{\Delta}{\omega} & 0 & 0 \\ -\frac{\Delta}{\omega} & 1 & 0 & 0 \\ 0 & 0 & 1 & \frac{\Delta}{\omega} \\ 0 & 0 & \frac{\Delta}{\omega} & 1 \end{pmatrix} \quad (12)$$

with the ordinary dimensionless BCS density of states $\rho_s(\omega) = |\omega|\theta(|\omega|-\Delta)/\sqrt{\omega^2-\Delta^2}$. It is straightforward to show that the tunneling current reads²⁰

$$J = J_N + J_A \quad (13)$$

with

$$J_N = \frac{e}{h} \int d\omega [f_l(\omega - eV) - f_r(\omega)] \sum_{i=1,3} [G_d^r \Gamma_s G_d^a \Gamma_f]_{ii} \quad (14)$$

and

$$J_A = \frac{e}{h} \int d\omega [f_l(\omega - eV) - f_l(\omega + eV)] \sum_{i=1,3}^{j=2,4} G_{d,ij}^r (\Gamma_f G_d^a \Gamma_f)_{ji}, \quad (15)$$

where $f_l(\omega)$ and $f_r(\omega)$ are the Fermi-distribution functions in the left and right leads, respectively. J_N is the normal tunneling current which is caused by the single quasiparticle or quasihole transport, and J_A is the Andreev reflection current. We can show that, in the linear-response regime, the normal tunneling conductance and the AR conductance are obtained as follows:

$$G_N = \frac{e^2}{h} \int d\omega \left[-\frac{\partial f}{\partial \omega} \right]_{i=1,3} \sum [G_d^r \Gamma_s G_d^a \Gamma_f]_{ii} \quad (16)$$

and

$$G_A = \frac{2e^2}{h} \int d\omega \left[-\frac{\partial f}{\partial \omega} \right]_{i=1,3}^{j=2,4} \sum G_{d,ij}^r (\Gamma_f G_d^a \Gamma_f)_{ji}. \quad (17)$$

Since the normal linear conductance is zero, $G_N = 0$, at zero temperature, only the Andreev reflection process contributes to the linear electronic transport of the system. So the total conductance G is equivalent to G_A .

III. THE CALCULATION AND DISCUSSION

We discuss the linear AR conductance at zero temperature for the F-QD-S, in which the energy level of the QD controlled by the gate voltage V_g is restricted in the range of the energy gap of the S-lead, that is, $|\varepsilon_d| < \Delta$ and $|\varepsilon_d \pm R| < \Delta$. In the following calculations, both Fermi energies of the F- and S-leads are set to zero. The energy gap of the S-lead, Δ , is taken as the energy unit and the spin polarization is chosen as $P = 0.3$.

First we illustrate the effect of the intradot spin-flip scattering on resonant behaviors of the AR conductance versus

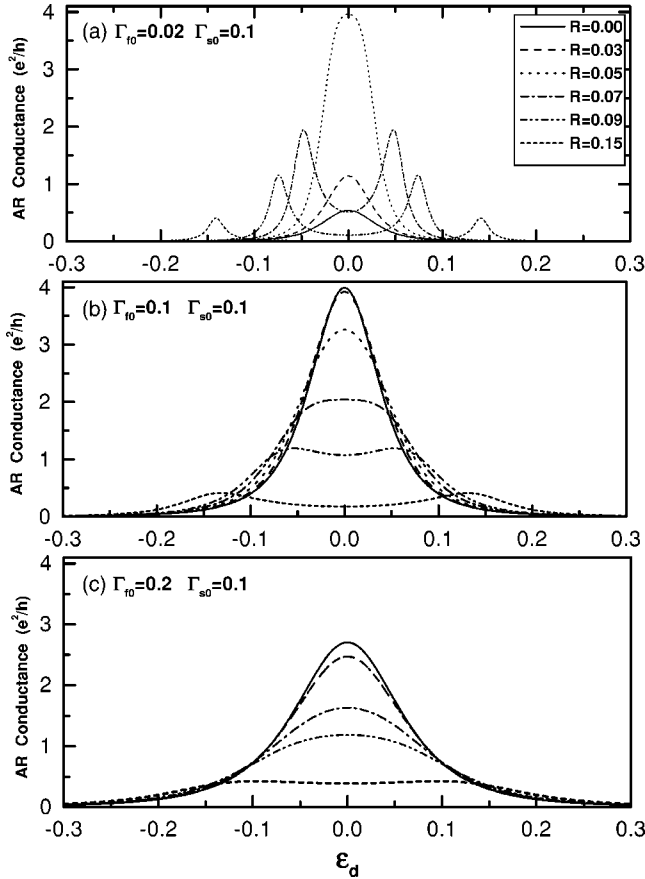


FIG. 2. The resonant curves of the AR conductance vs the energy level of the QD, ε_d , with parameters $P=0.3$, $\Gamma_{s0}=0.1$, and several spin-flip scattering strengths $R=0$ (solid line), 0.03 (dashed line), 0.05 (dotted line), 0.07 (dot-dashed line), 0.09 (dot-dot-dashed line), and 0.15 (short dashed line) for three different spin-averaged tunneling couplings to the F-lead: (a) $\Gamma_{f0}=0.02$, $\Gamma_{f0} < \Gamma_{s0}$; (b) $\Gamma_{f0}=0.1$, $\Gamma_{f0}=\Gamma_{s0}$; and (c) $\Gamma_{f0}=0.2$, $\Gamma_{f0} > \Gamma_{s0}$.

the energy level of the QD ε_d . For a fixed $\Gamma_{s0}=0.1$, we plotted the AR conductance as a function of ε_d in Figs. 2(a)–2(c) with $\Gamma_{f0}=0.02$, $\Gamma_{f0}=0.1$, and $\Gamma_{f0}=0.2$, respectively. Different spin-flip scattering strength curves for $R=0$ (solid line), 0.03 (dashed line), 0.05 (dotted line), 0.07 (dot-dashed line), 0.09 (dot-dot-dashed line), and 0.15 (short dashed line) are shown. In Fig. 2(a), where $\Gamma_{f0} < \Gamma_{s0}$, for a weak spin-flip scattering strength in the range of $R=0$ –0.05, the AR conductance displays a single-peak resonance at $\varepsilon_d=0$ and its amplitude gradually rises until the maximum $G_m=4e^2/h$ at $R_m \approx \Gamma_{s0}/2=0.05$ with R increasing. This is a perfect AR tunneling process. For some stronger spin-flip scatterings $R \in (0.05 \sim 0.06)$, the AR conductance displays also a single-peak profile at $\varepsilon_d=0$, but the amplitude of the resonant peak reduces quickly. Further increasing the spin-flip scattering strength, $R > 0.065$, for instance, the original single-peak conductance develops to a well-resolved double-peak resonance with the peaks near $\varepsilon = \pm R$, respectively. It is also shown that the intradot spin-flip scattering always suppresses the heights of the resonant double peaks.

Figure 2(b) presents the curves of the resonant AR conductance for the tunneling couplings, $\Gamma_{f0}=\Gamma_{s0}=0.1$, and the

other parameters are the same as those in Fig. 2(a). Similar AR conductance behaviors have been indicated. But, comparing with Fig. 2(a), only a strong enough spin-flip scattering ($R > 0.08$, for instance) can lead to a double-peak resonance of the conductance due to the larger broadening of the two split levels $\Gamma=(\Gamma_{f0}+\Gamma_{s0})$ in this case. Also, we find that the width of the resonant double peak enlarges because of the enhanced broadening of the minority spin, $\Gamma_{f\downarrow}$. In Fig. 2(c), where $\Gamma_{f0} > \Gamma_{s0}$, the amplitude of the single-peak resonance shows a novel feature: as the spin-flip scattering increases, the amplitude of the resonance peak decreases monotonously. It is believed that in the presence of the intradot spin-flip scattering, the amplitude of the single peak of the AR conductance embodies characteristic behaviors that depend essentially on the effective overlap of the broadening of the two split levels.

To elucidate the evolution of the AR conductance from single-peak to double-peak resonance, we calculate the magnitude of the AR conductance $G_0(R)$ as a function of the spin-flip scattering strength R at $\varepsilon_d=0$. Define the ratio of the two tunneling coupling strengths $r=\Gamma_{s0}/\Gamma_{f0}$. The matching condition of the Fermi velocity,¹³ $\Gamma_{f\uparrow}\Gamma_{f\downarrow}=\Gamma_{s0}^2$, now reads $P^2+r^2=1$. This matching condition is analogous to the one initially formulated in bulk F-S systems $k_{f\uparrow}k_{f\downarrow}=k_s^2$,^{8,9} which is related to the electron occupation in the structure of the system. Figure 3(a) shows curves of the AR conductance G_0 , for a given $\Gamma_{s0}=0.1$ and several different coupling strengths $\Gamma_{f0}=0.1$ (solid line), 0.1/3 (dashed line), 0.1/5 (dotted line), 0.1/7 (dot-dashed line), and 0.1/9 (dot-dot-dashed line). Remarkably, for the case of $r > 1$, the magnitude of G_0 increases first to its maximum $4e^2/h$ at R_m and then drops quickly as the spin-flip scattering strength R increases. It should be mentioned that for $r > 1$ where the matching of the Fermi velocity can never be satisfied, G_0 should decrease monotonously with the spin polarization P increasing and could not reach its maximum $4e^2/h$ in F-S junctions^{8,9} and in the F-QD-S system.^{13,14} Our calculations indicated that there must exist, apart from what is considered in Refs. 13 and 14, other mechanisms that result in the perfect AR tunneling with G_0 of $4e^2/h$. We believe that the intradot spin-flip scattering may account for it, which we will discuss further later in the paper. For a small enough Γ_{f0} , G_0 becomes very sharp, and the maximum position R_m approaches very closely to $\Gamma_{s0}/2$. This means that once the spin-flip scattering strength slightly deviates from $\Gamma_{s0}/2$, the AR conductance drops from $4e^2/h$ to 0 quickly.

The typical feature shown in Fig. 3(a) is understood qualitatively as follows. Spin-up and spin-down electrons can escape from the QD through the tunneling to the leads, which leads to the resonant broadening of the two spin-coherent split levels ($\varepsilon_d = \pm R$) by an amount of Γ . Here the linewidth of the split levels, $\Gamma=(\Gamma_{f0}+\Gamma_{s0})$, delineates the distribution of the density of states (DOS) qualitatively. When $R < R_m$ ($\approx \Gamma_{s0}/2$), the linewidths of the two split levels are overlapped effectively at $\varepsilon_d=0$, so that the AR conductance versus ε_d behaves as a single-peak resonance. In this situation, the AR conductance G_0 is enhanced with increasing R because the intradot spin-flip scattering not only shifts the level position of the QD from $\varepsilon_d=0$ to $\varepsilon_d = \pm R$, but also changes

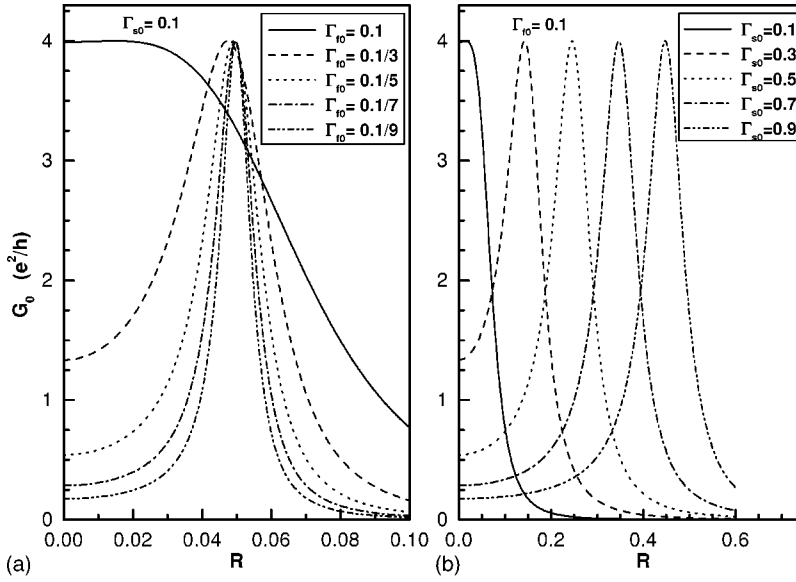


FIG. 3. The AR conductance vs the R at $\varepsilon_d = 0$ with $P=0.3$, $\Gamma_{f0} < \Gamma_{s0}$. (a) For fixed $\Gamma_{s0}=0.1$, and different $\Gamma_{f0}=0.1$ (solid line), $0.1/3$ (dashed line), $0.1/5$ (dotted line), $0.1/7$ (dot-dashed line), $0.1/9$ (dot-dot-dashed line). (b) For fixed $\Gamma_{f0}=0.1$, and different $\Gamma_{s0}=0.1$ (solid line), 0.3 (dashed line), 0.5 (dotted line), 0.7 (dot-dashed line), 0.9 (dot-dot-dashed line).

the spin-up and spin-down distribution of the DOS for the split levels.¹⁷ Since the minority spin population near the Fermi energy determines the probability of the pairing and thereby the behaviors of the AR tunneling, the spin-flip scattering that turns effectively the majority spin carriers to minority ones near $\varepsilon_d=0$ will cause G_0 to rise possibly to its maximum $4e^2/h$, at R_m , when spin-up and spin-down carriers from the F-lead form pairs into the S-lead completely. When $R > \Gamma_{s0}/2 + \Gamma_{f0} > R_m$, the two split levels have been separated sufficiently away from each other, leaving an almost vanishing spin-dependent DOS at $\varepsilon_d=0$. Therefore, $G_0(R)$ drops quickly to zero, resulting in a deep valley in the conductance curve at $\varepsilon_d=0$. This implies that the AR conductance has developed into a well-resolved double-peak resonance shown in Fig. 2(a). Figure 3(b) presents the curves of the AR conductance, G_0 versus R with a fixed $\Gamma_{f0}=0.1$, and different Γ_{s0} values with $r > 1$. The peak location R_m varies with Γ_{s0} , as expected, and the pattern for each curve is very analogous due to a constant spin minority $\Gamma_{f\downarrow}$ involved in the tunneling.

In Fig. 4(a), we plotted G_0 as a function of the spin-flip

scattering strength R with a fixed $\Gamma_{s0}=0.1$ and several different $\Gamma_{f0}=0.1$ (solid line), 0.3 (dashed line), 0.5 (dotted line), 0.7 (dot-dashed line), and 0.9 (dot-dot-dashed line). This is the situation of $r < 1$, and the magnitude of G_0 decreases monotonously with R increasing. Since the linewidths $\Gamma_{f\uparrow}$ and $\Gamma_{f\downarrow}$ are larger than Γ_{s0} , which is larger than the $\Gamma_{f\uparrow}$ and $\Gamma_{f\downarrow}$ in Fig. 3, the spin-up and spin-down DOS are relatively low compared with those in Fig. 3. With the increasing of spin-flip scattering that pushes the split level peaks farther away from $\varepsilon_d=0$, the minority spin occupation reduces significantly at $\varepsilon_d=0$. Simultaneously, the majority spin carriers can scarcely turn into the minority ones by the spin-flip scattering because a large $\Gamma_{f\uparrow}$ implies more uncertainty of the majority spin DOS and a lower probability for the pairing at $\varepsilon_d=0$. As a result, the magnitude of G_0 decreases monotonously with R increasing. In Fig. 4(b), we present some curves of G_0 for the case of $r < 1$ with a fixed $\Gamma_{f0}=0.1$, but for several different Γ_{s0} . Similar features, but an even faster drop in G_0 with R , compared with that in Fig. 4(a), have been indicated. As is well known, Γ_{s0} describes the probability

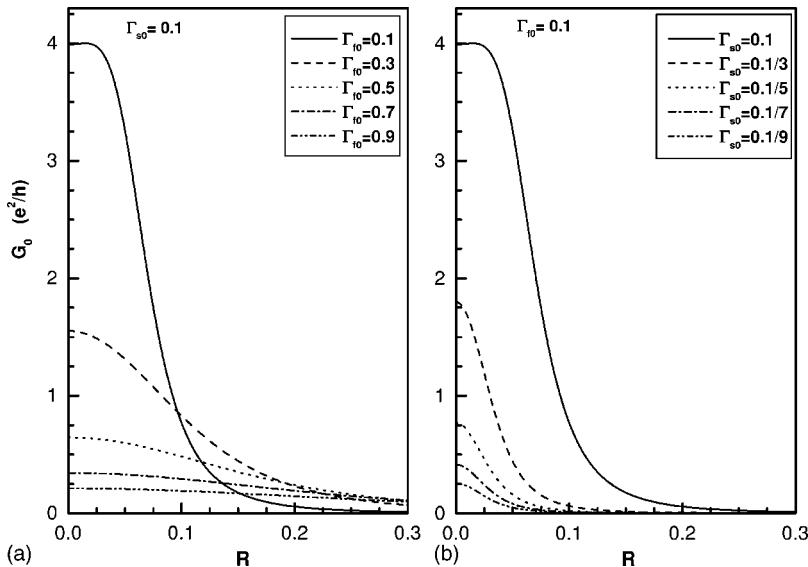


FIG. 4. The G_0 vs R with $P=0.3$, $\Gamma_{f0} > \Gamma_{s0}$. (a) For $\Gamma_{s0}=0.1$, and different $\Gamma_{f0}=0.1$ (solid line), 0.3 (dashed line), 0.5 (dotted line), 0.7 (dot-dashed line), 0.9 (dot-dot-dashed line). (b) For $\Gamma_{f0}=0.1$, and $\Gamma_{s0}=0.1$ (solid line), $0.1/3$ (dashed line), $0.1/5$ (dotted line), $0.1/7$ (dot-dashed line), $0.1/9$ (dot-dot-dashed line).

that two electrons in the QD tunnel into the S-lead forming a Cooper pair. So the weaker the Γ_{s0} , the lower the probability, and the faster G_0 drops to zero as R increases.

IV. CONCLUSION

We studied the spin-dependent AR tunneling through an F-QD-S structure by using the nonequilibrium Green function method. We found that the coherent spin-flip scattering in the QD plays important roles in the spin-dependent AR tunneling through the F-QD-S system. The observed behaviors of the AR conductance, a single- or double-peak resonance, versus the gate voltage are a consequence of the competition between the intradot spin-flip scattering and the resonant broadening of the two split levels because of the tunneling between the QD and the F/S lead(s). When the spin-flip scattering strength is smaller than the broadening of the split levels, the AR conductance exhibits a single-peak resonance. In this case, as the spin-flip scattering strength

increases, the height of the single peak conductance may first increase gradually and then drops quickly. However, when the spin-flip scattering induced splitting of the spin-degenerate level overwhelms the broadening of the split levels, the AR conductance appears as a symmetric double-peak resonance, for which a novel structure in the tunneling spectrum of the AR conductance is predicted to appear. We expect the present results may have practical applications in the field of spintronics.

ACKNOWLEDGMENTS

The authors are grateful to Qing-feng Sun for meaningful discussion and help. This work was supported by the National Natural Science Foundation of China (Grant No. 60371033) and by Shanghai Leading Academic Discipline Program, China. It was also supported by the Natural Science Foundation of China (NSFC) under Projects No. 90206031, and the National Key Program of Basic Research Development of China (Grant No. G2000067107).

*Email address: ymshi@mail.shu.edu.cn

- ¹W. Poirier, D. Mailly, and M. Sanquer, *Phys. Rev. Lett.* **79**, 2105 (1997).
- ²A. F. Morpurgo, B. J. Van Wees, T. M. Klapwijk, and G. Borghs, *Phys. Rev. Lett.* **79**, 4010 (1997).
- ³S. K. Upadhyay, A. Palanisami, R. N. Louie, and R. A. Buhrman, *Phys. Rev. Lett.* **81**, 3247 (1998).
- ⁴S. Gueron, M. M. Deshmukh, E. B. Myers, and D. C. Ralph, *Phys. Rev. Lett.* **83**, 4148 (1999).
- ⁵G. Prinz, *Science* **282**, 1660 (1998); S. A. Wolf *et al.*, *ibid.* **294**, 1488 (2001).
- ⁶M. J. M. de Jong and C. W. J. Beenakker, *Phys. Rev. Lett.* **74**, 1657 (1995).
- ⁷R. J. Soulen *et al.*, *Science* **282**, 85 (1998).
- ⁸I. Žutić and A. D. Sarma, *Phys. Rev. B* **60**, R16 322 (1999).
- ⁹I. Žutić and O. T. Valls, *Phys. Rev. B* **60**, 6320 (1999); **61**, 1555 (2000).
- ¹⁰R. Meservey and P. M. Tedrow, *Phys. Rep.* **238**, 173 (1994).
- ¹¹G. E. Blonder, M. Tinkham, and T. M. Klapwijk, *Phys. Rev. B* **25**, 4515 (1982).
- ¹²Y. Zhu, Q. F. Sun, and T. H. Lin, *Phys. Rev. B* **69**, 121302 (2004).
- ¹³Y. Zhu, Q. F. Sun, and T. H. Lin, *Phys. Rev. B* **65**, 024516 (2001).
- ¹⁴A. F. Feng and S. J. Xiong, *Phys. Rev. B* **67**, 045316 (2003).
- ¹⁵A. V. Khaetskii and Y. V. Nazarov, *Phys. Rev. B* **61**, 12 639 (2000); A. V. Khaetskii, *Physica E (Amsterdam)* **10**, 27 (2001).
- ¹⁶W. Rudzinski and J. Barnaś, *Phys. Rev. B* **64**, 085318 (2001); F. M. Souza, J. C. Egues, and A. P. Jauho, *cond-mat/0209263* (unpublished).
- ¹⁷P. Zhang, Q. K. Xue, Y. P. Wang, and X. C. Xie, *Phys. Rev. Lett.* **89**, 286803 (2002).
- ¹⁸R. López and D. Sánchez, *Phys. Rev. Lett.* **90**, 116602 (2003).
- ¹⁹J. Ma and X. L. Lei, *cond-mat/0309520* (unpublished); B. Dong, H. L. Cai, S. Y. Liu, and X. L. Lei, *J. Phys.: Condens. Matter* **15**, 8435 (2003).
- ²⁰Z. Y. Zeng, F. Claro, and Baowen Li, *cond-mat/0110502* (unpublished).